# Decentralized PID control with inverted decoupling and superheating reference generation for efficient operation: Application to the Benchmark PID 2018

**J. Garrido**, M. Lara*, M. L. Ruz*, F. Vázquez*, J. A. Alfaya****
**F. Morilla*****

**Computer Science and Numerical Analysis Department, University of Cordoba, 14071 Cordoba, Spain (Tel: 34-357-218729; e-mail: juan.garrido@uco.es, p12laorm@uco.es, mario.ruz@uco.es and fvazquez@uco.es), **Systems Engineering and Automatic Control Department, University of Sevilla, 41092, Sevilla, Spain (e-mail: jalonso9@us.es) ,***Computer Science and Automatic Control Department, UNED, Madrid, Spain (e-mail: fmorilla@dia.uned.es)*

**Abstract:** This paper deals with the control problem of a refrigeration vapor compression system proposed as a benchmark for the IFAC Conference on Advances in PID Controllers (PID'18). This refrigeration system is a multivariable nonlinear process that shows interactions and is subjected to input constraints. In this work, a decentralized PID control with inverted decoupling is proposed as control structure. The inverted decoupling is designed from an approximated multivariable linear model. Then, the PID controllers are tuned by genetic algorithms to minimize a performance index. In addition, a superheat reference generation is developed to achieve stationary operation points with maximum coefficient of performance which is a widespread efficiency measurement in these systems. Simulations considered in the benchmark show that the proposed design achieves better performance than the reference case.

*Keywords:* vapor compression refrigeration cycle, decoupling control, PID control, optimal operation.

## 1. INTRODUCTION

The vapor compression refrigeration cycle (VCRC) is the leading technology in cooling generation for household, commercial and industrial applications such as temperature control of buildings and automobiles for human comfort, or domestic and supermarket refrigerators for food storage and transportation (Wark, 2000). These refrigeration processes lead to huge energy consumption and have an important economic and environmental impact as it is supported by several studies (Zhao et al., 2013). The improvement of the energy efficiency of VCRC systems through process control and optimization is a key problem due to global warming and energy shortage concerns (Kim et al., 2011). Mostly VCRC systems consist of four main elements: two heat exchangers (evaporator and condenser), an expansion valve and a compressor. The heat is transferred by the refrigerant from a space of lower temperature (cold reservoir) or from the evaporator secondary fluid to an environment of high temperature (hot reservoir) or to the condenser secondary fluid. Generally, there are two manipulated variables to operate the system: the compressor speed and the opening degree of the expansion valve. The secondary mass flows and their inlet temperatures at evaporator and condenser act as disturbances. These systems are multivariable processes showing interactions and nonlinear dynamics under a wide range of operating conditions. In recent years, many researchers have paid attention to the control of VCRC systems using different approaches, such as decentralized PID control (Marcinichen et al., 2008), decoupling multivariable control (Shen et al., 2010), model predictive control (Ricker, 2010), and robust control (Bejarano et al., 2015).

There are two approaches of centralized control: a pure centralized strategy (Wang et al., 2003), or a decoupling network D(s) combined with a diagonal decentralized controller C(s) (Cai et al., 2008). The last of them uses the decoupling network to reduce the existing process interaction, allowing for independent control of the loops. The controller C(s) sees the apparent process $Q(s)=G(s)\cdot D(s)$ as a set of completely independent processes. Most decoupling approaches use a conventional decoupling scheme in which the process inputs are derived by a time-weighted combination of feedback controller outputs. In this case, the decoupler design is obtained from (1), generally specifying two elements of the decoupler or the two desired transfer functions of the apparent process. The most extended forms of conventional decoupling are termed ideal and simplified decoupling.

$$D(s) = G^{-1}(s)\cdot Q(s) \quad (1)$$

An alternative structure is inverted decoupling, that derives a process input as a time-weighted combination of one feedback controller output and the other process inputs (Fig. 1). In this case, it is possible to keep the same apparent process of ideal decoupling while using the simple decoupler elements of simplified decoupling (Garrido et al., 2011a). In (Garrido et al., 2011b), the main practical advantages of this scheme are studied in detail.

 

This paper illustrates the application of a decentralized PID control in combination with inverted decoupling to the refrigerant system considered in the benchmark problem for the IFAC Conference on Advances in PID Controllers (PID'18). Additionally, it is demonstrated that the process efficiency can be improved by means of a generator of optimal superheat set-points according to the operation conditions. In section 2, some aspects of the VCRC system are commented, and a linearized model is presented for performing the control design. The methodology of decentralized PID control with inverted decoupling is discussed in section 3. In section 4, it is explained how to determine the superheat references so that the system is operated in a more efficient way. In section 5, the proposed designs are applied to the benchmark and the results are evaluated. Finally, section 6 summarizes the conclusions.

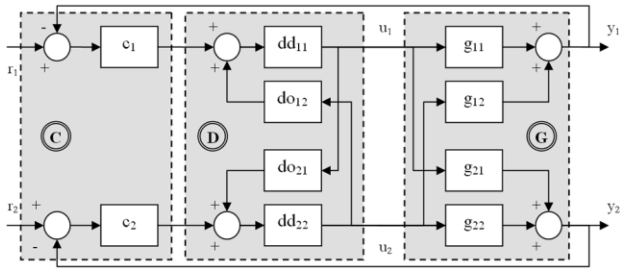


Fig. 1. 2x2 generalized inverted decoupling scheme.

## 2. THE REFRIGERATION SYSTEM

This work is focused on the VCRC control problem associated to the proposition in the benchmark PID 2018. In this case, the refrigerant process can be approached as a multivariable system with two variables (the outlet temperature of the evaporator secondary flux $T_{e,sec,out}$ and the superheating of the refrigerator at the evaporator outlet SH) that can be controlled by two manipulated variables (compressor speed N and expansion valve opening $A_v$). There are several disturbance variables; however, only the inlet temperature of the evaporator secondary flux $T_{e,sec,in}$ and the inlet temperature at the condenser secondary flux $T_{c,sec,in}$, are considered in this work. The input variable $A_v$ is subjected to the range of [10-100] %, and N, to the range of [30-50] Hz. More information about the refrigerant model can be found in http://servidor.dia.uned.es/~fmorilla/benchmarkPID2018.

In order to carry out the proposed design, it is necessary to start from a linear model of the plant. Since the nonlinearity of VCRC system, their approximated linear models vary considerably depending on the operational point. In this work, an average linear model is obtained from the approximated linear models obtained at the four operation conditions considered in the benchmark simulation according to the disturbance and reference values. The linear models are identified using the Matlab identification toolbox. The final continuous model is given by (2), where G(s) is the transfer matrix relating the vector of controlled variables ($T_{e,sec,out}$ and SH, respectively) to the vector of manipulated variables ($A_v$ and N, respectively), and where $G_d(s)$ relates the controlled variables to the vector of disturbance variables ($T_{e,sec,in}$ and $T_{c,sec,in}$, respectively). The other disturbances are not identified because they will not be taken into account.

$$G(s)=\begin{pmatrix}\dfrac{-0.0376\cdot(s+0.0165)}{s+0.0274} & \dfrac{-2.8558\cdot10^{-4}}{s+0.1387}\\ \dfrac{-0.4505\cdot(s+0.2642)}{s+0.0361} & \dfrac{0.1922\cdot(s+0.4141)}{s+0.0462}\end{pmatrix}$$
$$G_d(s)=\begin{pmatrix}0.9825 & \dfrac{0.0084}{s+0.0429}\\ 0.6584 & \dfrac{0.0549}{s+0.0403}\end{pmatrix} \quad (2)$$

The open loop dynamics of this model are stable for all the inputs and disturbances. The diagonal elements of the relative gain array (RGA) (Bristol, 1966) of G(s) has a value of 0.85. This indicates that the process has a moderate interaction and it recommends the input-output pairing in which the variable $T_{e,sec,out}$ is controlled by the expansion valve, and the superheating by the compressor. This is not the typical pairing in most VCRC systems, where the superheating is regulated by the expansion valve; however, the recommended pairing will be employed in the rest of the paper.

## 3. PID CONTROL WITH INVERTED DECOUPLING

### *3.1 Inverted decoupling*

Considering the unity output feedback 2x2 control scheme in Fig. 1, and assuming that the open loop transfer matrix of the apparent process Q(s)=G(s)·D(s) should be diagonal, the elements of the inverted decoupling are given by

$$dd_{11}=\frac{q_1}{g_{11}} \qquad do_{12}=\frac{-g_{12}}{q_1} \qquad do_{21}=\frac{-g_{21}}{q_2} \qquad dd_{22}=\frac{q_2}{g_{22}}, \quad (3)$$

where the Laplace variable has been omitted, and where $q_1(s)$ and $q_2(s)$ are the desired apparent open loop transfer functions. The proof can be found in (Garrido et al., 2011a). The main advantage of (3) is the simplicity of the decoupler elements in comparison with that of the elements in (4), obtained with a conventional decoupling scheme.

$$D=\begin{pmatrix}d_{11} & d_{12}\\ d_{21} & d_{22}\end{pmatrix}=\frac{\begin{pmatrix}g_{22}q_1 & -g_{12}q_2\\ -g_{21}q_1 & g_{11}q_2\end{pmatrix}}{g_{11}g_{22}-g_{12}g_{21}} \quad (4)$$

The decoupler elements of (3) do not contain sum of transfer functions, whereas the decoupler elements of (4) may result very complicated even if the elements of the system have simple dynamics. In addition, the apparent processes $q_i(s)$ may keep very simple in such a way that simple tuning rules can be used for the decentralized controller. Nevertheless, the structure of inverted decoupling control presents an important disadvantage: because of stability problems, it cannot be applied to processes with multivariable right half plane (RHP) zeros, that is, RHP zeros in the determinant of G(s). Fortunately, the linear model in (2) does not have such RHP zeros, so this method can be applied.

In order to obtain the decoupler elements, it is only necessary to specify the two transfer functions $q_i(s)$. They can be

selected freely as long as the controller elements are realizable. The realizability conditions for inverted decoupling are well discussed in (Garrido et al., 2011a). Usually, the two elements in the direct way ($dd_{11}(s)$ and $dd_{22}(s)$) are fixed to one for easiness of implementation. This implies that the apparent processes $q_i(s)$ are given by the diagonal elements of G(s). For the system under study, and after selecting the desired apparent diagonal process Q(s) as the diagonal elements of G(s) in (2), the following decoupling elements are achieved:

$$\begin{aligned} dd_{11}(s) &= dd_{22}(s) = 1 \\ do_{12}(s) &= \frac{-0.0076\cdot(s+0.0274)}{(s+0.1387)\cdot(s+0.0165)} \\ do_{21}(s) &= \frac{2.343\cdot(s+0.0264)\cdot(s+0.0462)}{(s+0.0361)\cdot(s+0.0414)} \end{aligned} \quad . \tag{5}$$

*3.2 PID controllers*

The decentralized control proposed in this work is composed by two PID controllers using a standard non-interactive structure as follows:

$$u(s) = Kp\cdot\left( a\cdot r(s) - y(s) + \frac{r(s)-y(s)}{Ti\cdot s} + \frac{Td\cdot s}{\alpha\cdot Td\cdot s+1}(b\cdot r(s)-y(s)) \right), \tag{6}$$

where u(s) is the control signal, r(s) the reference, y(s) the controlled signal, Kp is the proportional gain, Ti is the integral time constant, Td is the derivative time constant, and α is tuned to filter the derivative action. This continuous control law is implemented in a discrete time approximation using the Tustin algorithm. The proportional P(k), integral I(k) and derivative D(k) actions of this implementation in the k-th iteration are detailed below:

$$\begin{aligned} P(k) &= Kp\cdot(a\cdot r(k) - y(k))) \\ I(k) &= I(k-1) + Kpi\cdot(r(k) - y(k) + r(k-1) - y(k-1)) \\ D(k) &= -cd\cdot D(k-1) + Kpd\cdot(b\cdot(r(k) - r(k-1)) - y(k) + y(k-1)) \end{aligned} \quad , \tag{7}$$

where y is the controlled variable and r is the reference. The constants Kpi, Kpd and cd are given by:

$$Kpi = Kp\cdot\frac{h}{2\cdot Ti} \quad Kpd = Kp\cdot\frac{2\cdot Td}{h+2\alpha\cdot Td} \quad cd = \frac{h-2\alpha\cdot Td}{h+2\alpha\cdot Td}, \tag{8}$$

where h is the sample time. The control signal is the sum of these three actions and, additionally, a feedforward action F(k) which can be provided by feedforward or decoupling elements. Therefore, the control signal is given by u(k)=P(k)+I(k)+D(k)+F(k). The parameters a and b in (5) and (7) are set-point weights (Aström and Hägglund, 2006) and can be used to avoid large control signals due to sudden set-point changes. The controller with a=0 and b=0 is called I-PD, and that with a=1 and b=0 is called PI-D. The case with both parameters equal to the unity is the conventional PID.

To cope with the input constraints of the process, an anti-windup mechanism is implemented using an input constraint model where their saturations are considered. When the final control signal u(k) is out of its limits, this mechanism updates the integral term I(k) constrained u(k) to the exceeded limit. In the I-PD controller, the algorithm for the case of surpassing the maximum saturation input is as follows:

$$\begin{aligned} &if\ u(k) > u_{\max} \\ &\quad I(k) = u_{\max} - P(k) - D(k) - F(k) \\ &end \\ &u(k) = P(k) + I(k) + D(k) + F(k) \end{aligned} \quad . \tag{9}$$

In this work, the PID controllers are configured as I-PD with a sample time of one second, and a feedforward input to add the decoupling actions. It is important to note that it is possible to use the commented simple monovariable strategy due to the structure of inverted decoupling. In the conventional decoupling scheme of Fig.1, it is more difficult to implement an anti-windup strategy because the final control signals are not fed back to the PID controllers (Garrido et al., 2011b).

*3.3 PID tuning using genetic algorithms*

The PID tuning procedure is performed by genetic algorithms (GA) simulating the approximated linear model in (2) under the same conditions of the standard test described in the benchmark. All variables involved in the linear model are turned into absolute variables adding the corresponding values in the initial operational point. For evaluation, the benchmark proposes a combined index composed of eight individual indices: the first two indices are the Ratios of Integrated Absolute Error (RIAE) of the controlled variables $T_{e,sec,out}$ and SH form their references. The third one is the Ratio of Integrated Time multiplied Absolute Error (RITAE) for $T_{e,sec,out}$, taking into account that the standard simulation only includes one sudden change in its reference. The fourth, fifth and sixth indices are the RITAE for SH, taking into account that the standard simulation includes three sudden changes in its reference. The seventh and eighth indices are the Ratios of Integrated Absolute Variation of Control signal (RIAVU) for the two manipulated variables. The combined index is obtained as the mean value of the eight individual indices using a weighting factor for each index.

Due to the nonlinearity of the combined performance index, the PID tuning design that minimizes this index can be formulated as a nonlinear optimization problem, and thus it can be solved using GA (Goldberg, 1989),(Wang and Kwok, 1994). The procedure is performed using the Global Optimization toolbox of Matlab. In each PID controller, there are four parameters to be adjusted: Kp, Ti, Td and α. The parameter search range is limited to $[10^{-4}, 30]$. For the Kp gain of the controller of $T_{e,sec,out}$ , this range is negative. The main options configured in the genetic algorithm are: a population size of 5000, elite count of 0.05 times the population size for reproduction with a crossover fraction of 0.8. After multiples simulations, the resultant PID parameters that achieve the best combined index are collected in Table 1. Using the linear model, a final index of 0.2464 is obtained; however, this value gets worse when using the original nonlinear model, as it will be shown later.

**Table 1. PID controller parameters**

| PID | Kp | Ti | Td | α |
|---|---|---|---|---|
| $T_{e,sec,out}$ - $A_v$ | -6.95 | 0.24 | 5.23 | 16.3 |
| SH - N | 2.23 | 0.39 | 12.66 | 5.6 |

## 4. EFFICIENT OPERATION OF THE SYSTEM

One of the main issues operating refrigeration systems consists of achieving the desired operation conditions whilst the power consumption is minimized (Ruz et al., 2017). In the benchmark, the control loop set-point of $T_{e,sec,out}$ is assumed to be not tuneable since it is considered as an imposed demand requirement. However, there could be other different references of SH that operate the plant in the same environmental and demand conditions although consuming different power. In this section, a second control proposal dealing with this problem is described. It consists of the controller proposed in the previous section together with a block generator of optimal superheating set-points.

The steady state information provided by the nonlinear model under different conditions on $T_{e,sec,out}$, $T_{e,sec,in}$ and $T_c$, is used for determining the optimal SH set-point that achieves the cooling demand working in the same imposed conditions and minimizing the electrical power consumption of the system. Traditionally, this effectiveness is measured by means of the coefficient of performance (COP), which is defined as

$$COP = \frac{Q_e}{W_{com}}, \tag{10}$$

where $Q_e$ is the energy transfer rate at the evaporator and $W_{comp}$ is the compressor power consumption. For same cooling power demand, higher COP values imply operating the plant with lower electrical power consumptions.

As example, the basis of the set-point generation procedure is explained for the particular disturbance values of $T_{e,sec,in}$=-20 ºC, and $T_c$=30 ºC. Fig. 2a shows the feasible operating region in the manipulated variable space ($A_v$ and N), where the edge points 1, 2, 3 and 4 are highlighted. Under the previous disturbance conditions and using the nonlinear model, the points of the edge of this region can be translated into the corresponding ones in the controlled variable space ($T_{e,sec,out}$ and SH), as it shown in Fig. 2b. This closed and convex region delimits the achievable region in this space.

The same region is translated into the COP-$T_{e,sec,out}$ space (Fig. 3a) and the COP-SH space (Fig.3b). Given a desired $T_{e,sec,out}$, the maximum achievable COP is identified in Fig. 3a. It is placed in the downer limit 2-1 of the feasible region, which corresponds again to the operation points with minimal compressor speed N. For a desired $T_{e,sec,out}$ = -22.15 ºC, the maximum achievable COP is about 1.077, as it is depicted in Fig. 3a with a red dashed arrow. Then, the corresponding point in the SH-COP space indicates the superheating reference that should be provided to the control system to operate with this maximum COP in stationary state. In the case shown in Fig. 3b, the resultant SH is about 13 ºC. This reference of SH can be directly identified in the downer edge of the feasible region in the controlled variable space of Fig. 3b for the desired $T_{e,sec,out}$, obtaining the same value.

The same process can be performed working under different disturbance conditions with similar results. Therefore, for a reference $T_{e,sec,out}$, the optimal SH set-point can be identified in the controlled variable space in the intersection with the edge 2-1 (where the compressor works at its minimal speed). Edges 3-2 and 1-4 should also be taken into account for extreme values of $T_{e,sec,out}$. In these cases, the SH set-point is calculated in the same manner. However, the compressor speed in points of these edges is over its minimum value.

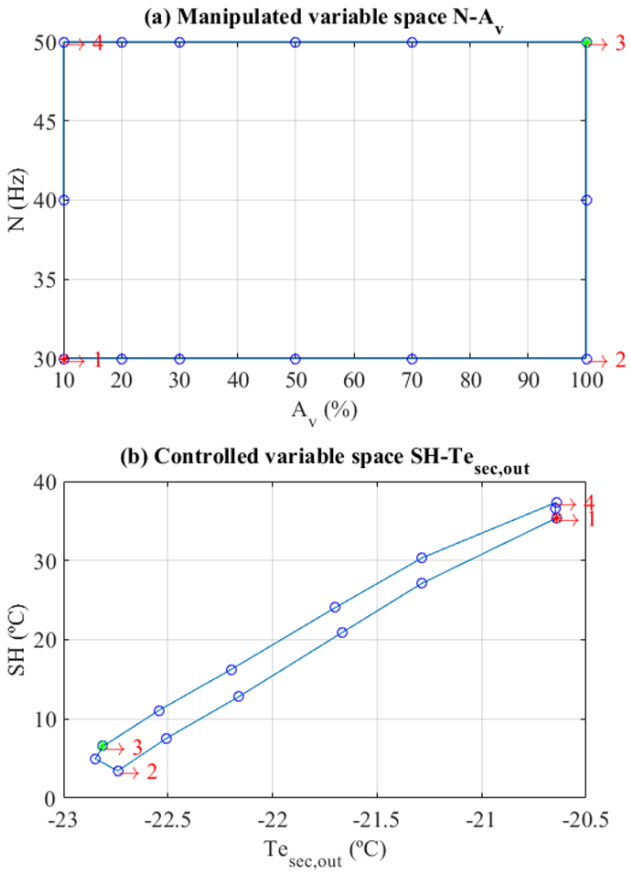


Fig. 2. (a) Manipulated variable space and (b) feasible region in the controlled variable space.

In this work, it is proposed to obtain the edges 3-2, 2-1 and 1-4 of the feasible region in the controlled variable space for different sets of disturbances values $T_{e,sec,in}$ and $T_{c,sec,in}$. For instance, Fig. 4 shows the edges corresponding to three disturbance cases: case A ($T_{e,sec,in}$=-20 ºC, $T_c$=30 ºC), case B ($T_{e,sec,in}$=-21 ºC, $T_c$=30 ºC), and case C ($T_{e,sec,in}$=-20 ºC, $T_c$=27 ºC). These cases correspond to the three different conditions simulated in the benchmark test.

Using these data, for given values of the two disturbances, the edge of interest in the controlled variable space is calculated by interpolation. Then, the optimal SH set-point is obtained from interpolation in this edge for a specified reference of $T_{e,sec,out}$. However, the minimal value of SH reference is limited to 2 ºC for the system safety, which is a common practice. In Fig. 5, the optimal SH set-points that arise in the benchmark are highlighted in the intersection with the two lines of references $T_{e,sec,out}$ = -22.15 ºC and $T_{e,sec,out}$ = -22.65 ºC. Fig. 5 shows the control system scheme of this proposal 2.

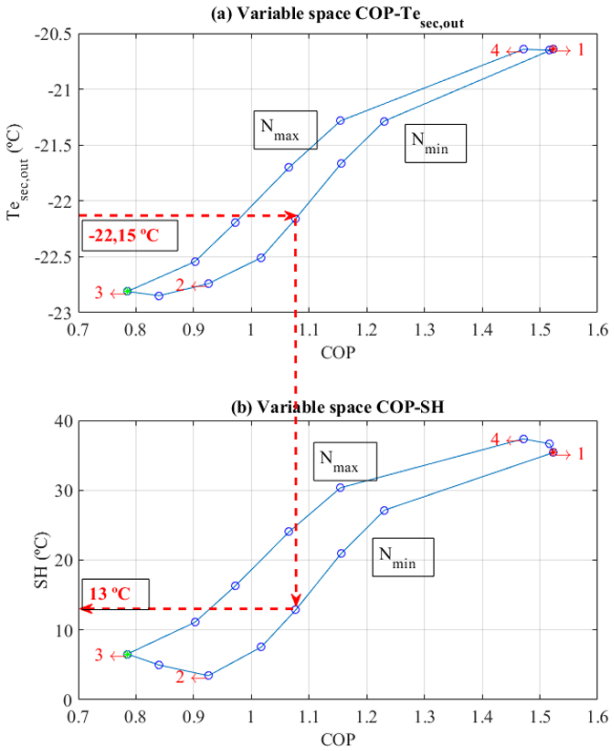


Fig. 3. Feasible region into the COP-$T_{e,sec,out}$ variable space (a) and COP-SH variable space (b).

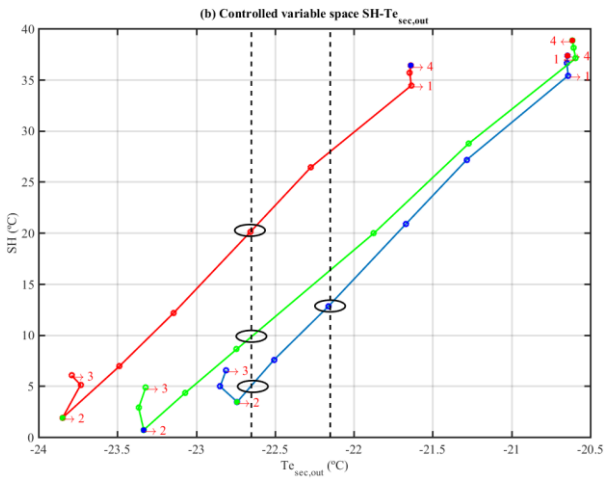


Fig. 4. Minimal COP operation edge of the feasible region in the controlled variable space for three different disturbance: case A (blue line), case B (red line) and case C (green line).

## 5. SIMULATION RESULTS

In this section, the performance of the proposed controllers is evaluated: the decentralized PID control with inverted decoupling described in Section 3 (Proposal 1), and this same control system with the previous procedure for generating superheating set-points (Proposal 2). Both proposals are tested for the benchmark using the nonlinear model and results are compared with the evaluated case presented in the benchmark. The same performance indexes of the benchmark are used for comparison with the proposal 1. The Individual performance indexes are listed in Table 2. Note that Proposal 2 is not included in the table, this is because the superheating set-point changes make the performance index comparison not applicable with respect to the reference case given in the benchmark. The proposed control 1 improves the global index (not shown in Table 2) with a value of **0.353** in comparison with the value of 0.682 of the evaluated controller illustrated in the benchmark. All indices related to the errors are improved at the expense of the control signals, where slightly higher values in the associated indices are obtained.

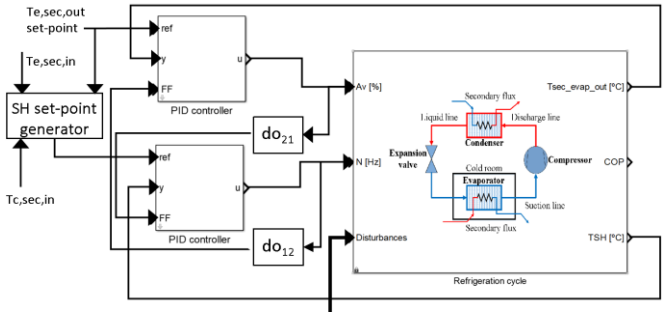


Fig. 5. Control system scheme for proposal 2.

**Table 2. Performance indexes**

| Index | $RIAE_1$ | $RIAE_2$ | $RITAE_1$ | $RITAE_{2t2}$ |
|---|---|---|---|---|
| Evaluated control | 0.351 | 0.446 | 1.610 | 0.183 |
| Proposed control 1 | 0.158 | 0.258 | 0.536 | 0.095 |
| **Index** | $RITAE_{2t3}$ | $RITAE_{2t4}$ | $RIAVU_1$ | $RIAVU_2$ |
| Evaluated control | 0.320 | 0.128 | 1.128 | 1.370 |
| Proposed control 1 | 0.186 | 0.113 | 1.338 | 1.431 |

The output signal and control signal responses of the proposed controllers are shown in Fig. 6 and Fig. 7, respectively. The evaluated control in the benchmark is also plotted as a reference case. The proposed control reaches the set-points and reject the disturbances very fast in comparison with the reference case. Simulating the proposed control 2, the references of superheating are different from those defined in the standard test because there is a block generating the set-points to operate the system. In this case, Fig. 7 shows that the compressor is working almost all the time at its minimal value of 30 Hz. Fig. 8 shows the COP of the proposed controllers. The proposed control 2 obtains the highest values of COP which implies energy savings and the consequent cost reduction and environmental enhancement.

## 6. CONCLUSIONS

In this work, a VCRC control problem, proposed as a benchmark, has been approached using a decentralized PID control with inverted decoupling. The methodology has been explained and applied to the process under review. This

methodology makes possible an easy design. In contrast to other conventional methods, thanks to the proposed decoupling scheme, other problems, like anti-windup, can be treated as in the monovariable case. This is not so simple for other conventional methods. The proposed control has been also complemented using a procedure to generate superheating set-points that allows to operate the system efficiently with optimal COP. After simulation, the effectiveness of the proposed designs is verified obtaining smaller performance indices than those of the reference case.

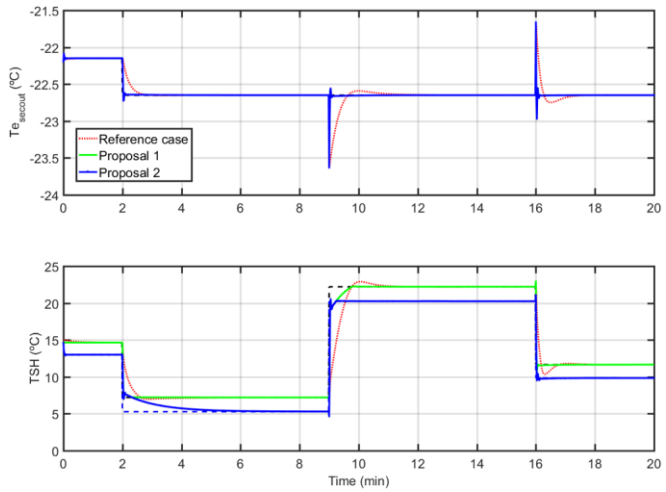


Fig. 6. Comparative simulation: controlled variables.

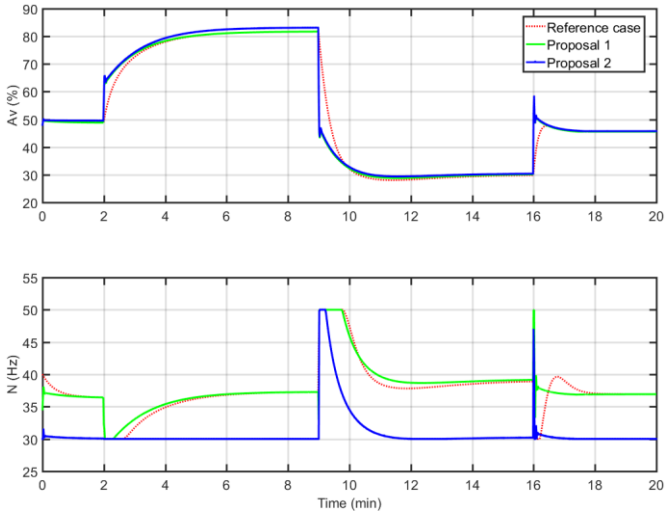


Fig. 7. Comparative simulation: manipulated variables.

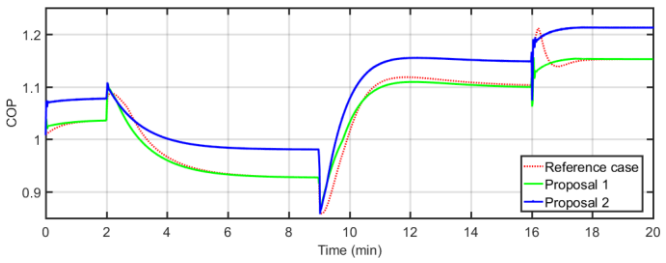


Fig. 8. Comparative simulation: COP.

ACKNOWLEDGEMENTS

This work was supported by the Spanish Ministry of Economy and Competitiveness [grant DPI2012-37580-C02-01]. This support is gratefully acknowledged.

REFERENCES

Åström, K.J., and Hägglund, T. (2006). *Advanced PID control*. ISA – The Instrumentation, System, and Automation Society.

Bejarano, G., Alfaya, J.A., Ortega, M.G. and Rubio, F.R. (2015). Multivariable analysis and $H_\infty$ control of a one-stage refrigeration cycle. *Appl. Therm. Eng*., 91, 1156-1167.

Bristol, E.H. (1966). On a new measure of interaction for multivariable process control, *IEEE Trans*, **11**, 133-134.

Cai, J., Ni, W., He, M.J. and Ni, C.Y. (2008). Normalized decoupling - A new approach for MIMO process control system design. *Ind. Eng. Chem. Res.* **47**, 7347-7356.

Garrido, J., Vázquez, F. and Morilla, F. (2011a). An extended approach of inverted decoupling. *Journal of Process Control* 21 (1), 55-68.

Garrido, J., Vázquez, F., Morilla, F., and Hägglund, T. (2011b). Practical advantages of inverted decoupling. *Proc. IMechE Part I: J. Systems and Control Engineering,* 225 (7), 977-992.

Goldberg, D.E. (1989). *Genetic Algorithms in Search, Optimization & Machine Learning*, Addison-Wesley.

Kim, M.H., Kim, J.H., Choi, A.S. and Jeong, J.W. (2011). Experimental study on the heat exchange effectiveness of a dry coil indirect evaporation cooler under various operating conditions. *Energy*, 36, 6479-6489.

Marcinichen, J., del Holanda, T., and Melo, C. (2008). A dual SISO controller for a vapor compression refrigeration system. In *12th Int. Refrig. and Air Cond. Conf., at Purdue, West Lafayette-IN, USA*.

Ricker, N.L. (2010). Predictive hybrid control of the supermarket refrigeration benchmark process. *Control Eng. Pract.*, 18(6), 608-617.

Ruz, M.L., Garrido, J., Vázquez, F., and Morilla, F. (2017). A hybrid modeling approach for steady-state optimal operation of vapor compression refrigeration cycles. *Appl. Therm. Eng*., 120, 74-87.

Shen, Y., Cai, W.J., and Li, S. (2010). Normalized decoupling control for high-dimensional MIMO processes for application in room temperature control HVAC systems. *Control Eng. Pract*., 18(6), 652-664.

Wang, P., Kwok, D.P. (1994). Optimal design of PID process controllers based on genetic algorithms, *Control Eng. Pract.*, 2(4), 641-648.

Wang, Q.W., Zhang, Y., and Chiu, M.S. (2003). None-interacting control design for multivariable industrial processes. *Journal of Process Control* 13 (3), 253-265.

Wark, k., Richards, D.E. (2000). *Thermodynamics* (6th ed.), William C Brown Pub (2000).

Zhao, L., Cai, W., Ding, X., Chang, W. (2013) Model-based optimization for vapor compression refrigeration cycle *Energy*, 55, 392-402.